



# Desertification Monitoring in the South-West of Iraqi Using Fuzzy Inference System

H.M. Abduljabbar<sup>1\*</sup>, A.J. Hatem<sup>2</sup>, A.A. Al-Jasim<sup>3</sup>

## Abstract

In this research, the region in the south-west of Iraq is classified using a fuzzy inference system to estimate its desertification degree. Three land cover indices are used which are the Normalized Difference Vegetation Index, Normalized Multi-Band Drought Index and the top of atmosphere surface temperature to build a fuzzy decision about the desertification degree using eight decision roles. The study covers a temporal period of 38 years, where about every 10 years a sample is elected to verify the desertification status of the region, starting from 1990 to 2018. The results show that the desertification status varied every 10 years, wherein 2000 encountered the highest desertification in the south-west of Iraq.

**Key Words:** Normalized Difference Vegetation Index, Normalized Multi-band Drought Index, Top of Atmosphere Temperature, South-west of Iraq.

**DOI Number:** 10.14704/nq.2020.18.5.NQ20160

**NeuroQuantology 2020; 18(5):01-11**

## Introduction

Desertification is extended kind of region degeneration which converts the prolific ecosystem to crisp one, by two decisive factors, namely environment, and human intervention [1]. It is one of the troubles and challenges which confront the human in the present time [2].

Sand dunes are in most of the central and southern regions of Iraq, this is due to lower rain full, higher temperature, increased solar radiation, and increased wind, which increased the evaporation rate at the expense of water intake as well as some human factors [3][4].

The climatic changes in Iraq generally and in the study area especially, helps in increased the desertification problem as well as the human factors and mismanagement to address the big problem, in spite of that multiple water sources of surface river water, groundwater and the rain, but

it has not been exploited well and efficiently in irrigating agricultural areas and many of which are based on old irrigating methods. This has exacerbated the problem, and increasing desertified areas, weak investment, and supporting agricultural activities in Iraq [3][4].

Given the wide scope of desertification, it is difficult to study this phenomenon in traditional methods of surface and field operations. Therefore, it is necessary to adopt modern techniques in the study of such phenomena widespread, which are the most important is the data of remote sensing and the provision of the satellite images that provide full coverage of the study area that helps to study the phenomenon in its real dimensions [5][6][7], and confirm the ability of remote sensing data to monitor and study the phenomenon of desertification [8][9].

**Corresponding author:** H.M. Abduljabbar

**Address:** <sup>1</sup>Department of Physics, College of Education for Pure Science Ibn-Al-Haitham, University of Baghdad, Baghdad, Iraq; <sup>2</sup>Department of Physics, College of Education for Pure Science Ibn-Al-Haitham, University of Baghdad, Baghdad, Iraq; <sup>3</sup>Department of Physics, College of Education for Pure Science Ibn-Al-Haitham, University of Baghdad, Baghdad, Iraq.

<sup>1</sup>E-mail: ali.a.n@ihcoedu.uobaghdad.edu.iq

<sup>2</sup>E-mail: hameed.m.aj@ihcoedu.uobaghdad.edu.iq

<sup>3</sup>E-mail: amal.j.h@ihcoedu.uobaghdad.edu.iq

**Relevant conflicts of interest/financial disclosures:** The authors declare that the research was conducted in the absence of any commercial or financial relationships that could be construed as a potential conflict of interest.

**Received:** 10 April 2020 **Accepted:** 06 May 2020



The most used indicators that are used to estimate and observe desertification are the Normalized Difference Vegetation Index (NDVI), which is vastly used to estimate vegetation conditions [10].

The NDVI is the ratio between the difference between the red and near-infrared band combination on the sum of the same bands [11][12]

$$NDVI = \frac{NIR-Red}{NIR+Red} \quad (1)$$

Which is used in estimating the yield of rice farms in southern Iraq using Landsat images [13][14].

The Normalized Multi-Band Drought Index (NMDI) where is used to monitor the soil's moisture content from space by using three bands (NIR, SWIR1, SWIR2).

NMDI is sensitive of soil and cultivates admixture was studied by Wang to expose that NMDI could be used to define moisture and water content status from space [13]

$$NMDI = \frac{NIR-(SWIR1-SWIR2)}{NIR+(SWIR1-SWIR2)} \quad (2)$$

The use of the fuzzy inference method to analyze data gives us the ability to deal with the imprecision that may exist naturally due to the complex nature of the system in question, and sometimes the digital data are vague and imprecision and here the fuzzy inference method provides a way to understand the behavior of the system through the interpolation process between input and the observed output states. Thus, the fuzzy inference models are characterized by high generality [15][16].

There are many kinds of research that used the FIS as a tool to study the soil such as, Hegde, S., In 2003, is study the land cover changes using the fuzzy inference system.

He uses the Landsat TM satellite's images as a source of information for the selected region of interest, the result showed that the classification accuracy using the FIS in better than traditional classification methods [17].

In 2004 Mohamed, A. and Hawas, Y., is studied the ability to determine the moisture content in sandy soil using neuro-fuzzy logic model, the results through their experiments reveal that their system is sensitive to the moisture content and ion

concentration and thereby able to calculate the moisture contained in the test soil samples [18].

Sharma, M. and et al, in 2011, is studying the effect of using different types of membership functions in a Mamdani fuzzy inference system on the classification accuracy of the satellite image, the results compared with the traditional classification method (Minimum distance and parallelepiped) and they found that the accuracy depends on the arrangement of the membership functions [19].

Shah, P. and Vayada, M.G., In 2015, is present a study to clarify the uncertainty in determining the class position and boundary and the similarity between different classes after classification. They use different classification methods and proposed the fuzzy logic classification method with detail and applied it to detect a water body in a satellite image [20].

Taufik, A. and Ahmad, S. In 2016, is classified a Landsat 8 image using fuzzy inference system by using land cover indices the parameters of the member function determined using Adaptive neuro-fuzzy inference system method, the results showed that the fuzzy inference system is effective and applicable on other Landsat areas [21].

In this research work, the desertification phenomena are monitored over 38 years. Due to the ambiguity of defining the desertification degree, a fuzzy inference system is adopted to determine the desert area and its desertification degree.

### Study Area Description

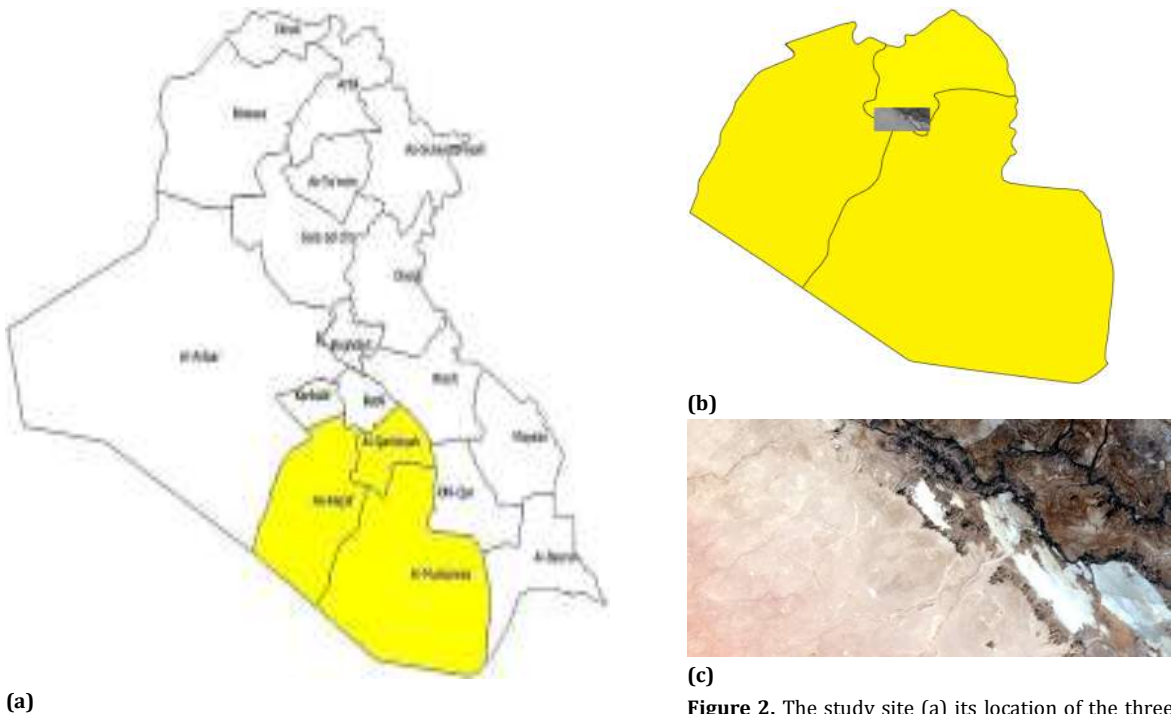
The study area is chosen because it represents the boundary between the desert region in the west of Iraq and the delta basin area of the Tigris and Euphrates rivers at the center of Iraq, sees Figure 1. Its located in the intersection of three provinces which are Al-Qādisiyyah, Al-Muthannā and An-Najaf, as illustrated in Figure 2.

Its covers approximately (1148.976 km<sup>2</sup>), within longitude range (44° 28' 30.63" to 44° 58' 51.72" E) and latitude range (31° 30' 34.40" to 31° 18' 2.10" N), as shown of natural color band combination in Figure 2c. The available remotely sensed data is downloaded from the website of the United States Geological Survey (USGS) Center for Earth recourses, observation and science [22].





Figure 1. The study site location on the Exploratory Soil Map of Iraq[23]



(a) (b) (c)  
Figure 2. The study site (a) its location of the three provinces on the map of Iraq (b) the location of the study site on the three provinces (c) True color of (Landsat-5 TM) study scene[22]



## Research Methodology

The desertification degree of the selected area is classified in a fuzzy manner based on the following approach.

1. Convert the satellite image bands numerical values to the top of atmosphere (TOA) reflectance and radiance coefficients, as follow[24]:

$$L_{\lambda} = M_L * Q_{cal} + A_L \quad (3)$$

$$\rho_{\lambda} = \frac{M_p * Q_{cal} + A_p}{\sin \theta} \quad (4)$$

Where:

$$L_{\lambda} = \text{Spectral radiance} \left( \frac{W}{m^2 \times str \times \mu m} \right)$$

$M_L$  = Radiance multiplicative scaling factor for the band.

$A_L$  = Radiance additive scaling factor for the band.

$Q_{cal}$  = pixel value in DN.

$\rho_{\lambda}$  = TOA Planetary Spectral Reflectance, without correction for the solar angle.  $M_p$  = Reflectance multiplicative scaling factor for the band.

$A_p$  = Reflectance additive scaling factor for the band.

2. Calculate the three-land cover indices for the study area, which are:
3. Normalized Difference Vegetation Index NDVI[12]

$$NDVI = \frac{NIR - Red}{NIR + Red} \quad (5)$$

*Red* = The red band

*NIR* = The Near Infrared band

- a. Normalize Difference Moisture Index NDMI[25]

$$NDMI = \frac{NIR - SWIR}{NIR + SWIR} \quad (6)$$

*SWIR* = The shortwave Infrared band

- b. Top of Atmosphere Temperature T[24]

$$T = \frac{K_2}{\log\left(\frac{K_1}{L_{\lambda}} + 1\right)} - 273 \quad (7)$$

*T* = TOA Brightness Temperature, in Celsius.

$K_1$  = Thermal conversion constant for the band.

$K_2$  = Thermal conversion constant for the band.

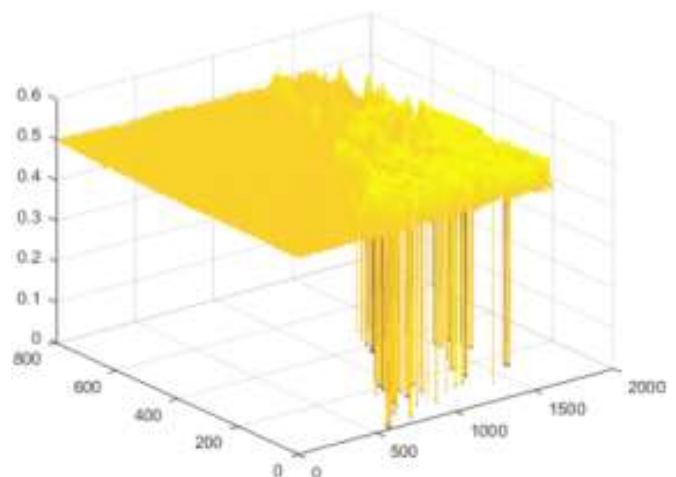
4. Define the active range for each land cover index.
5. Build a Mamdani fuzzy inference system with three input (the land cover indices) and

one output (the desertification decision value) based on eight decision roles.

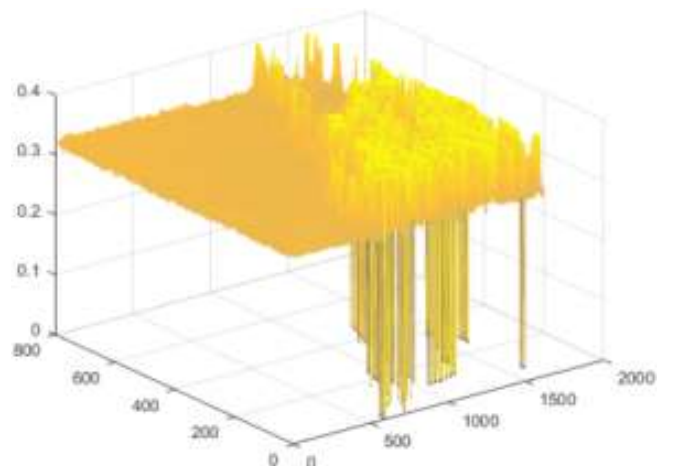
6. Apply the desertification decision value on the satellite land cover indices.

## Results and Dissuasion

This study covers the period from 1990 to 2018 with a sampling period of about every 10 years (1990, 2000, 2010 and 2018). The three land cover indices are calculated for four elected years. After converting the satellite digital number value to the equivalent reflectance and radiance values, the calculated three land cover indices after is illustrated in a 3D representation in the Figures 3-5. The thermal band (10.4–12.5  $\mu m$ )[26] of Landsat 5 and the thermal band number 10 (10.60–11.19  $\mu m$ )[27] of Landsat 8 are used to calculate the TOA temperature, where the value of the land cover indices for the water bodies is equal to zero.

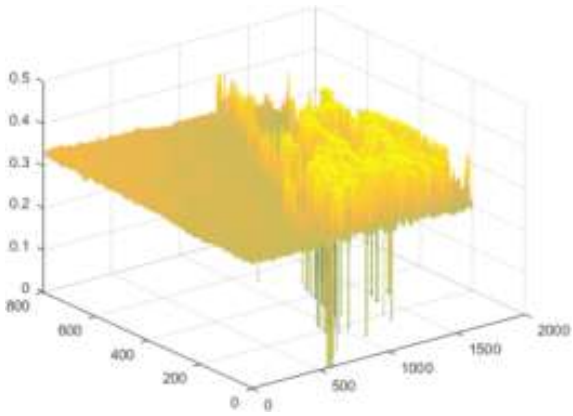


1990

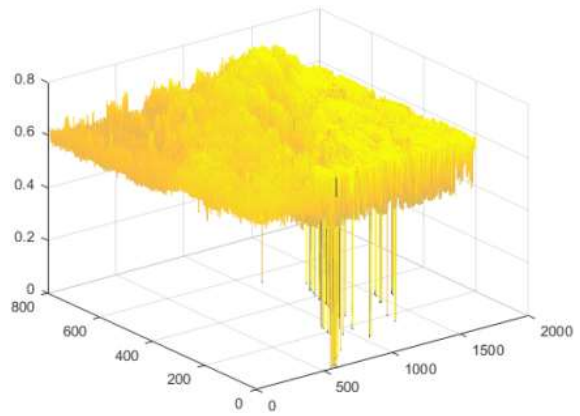


2000

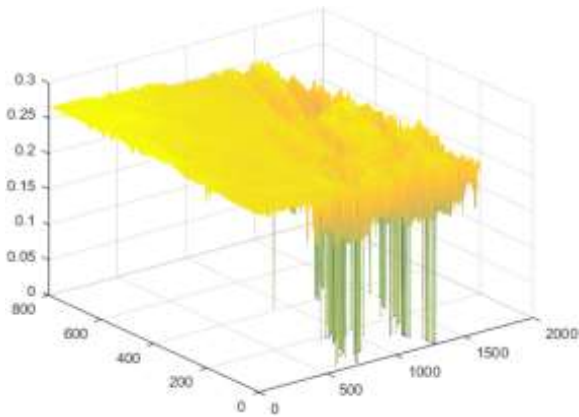




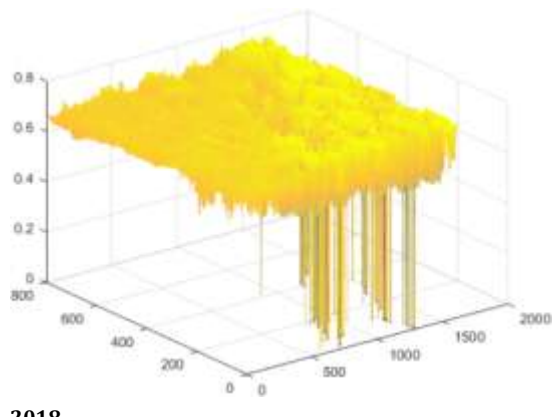
2010



2010



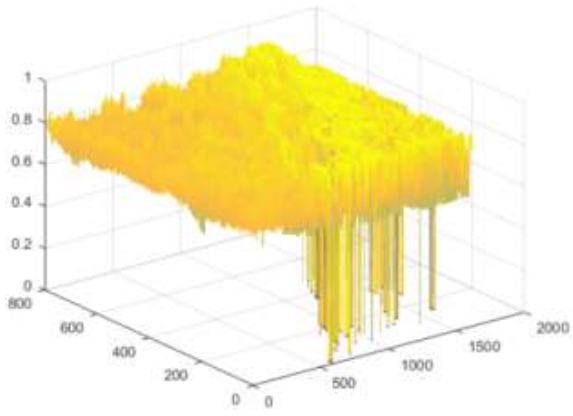
2018



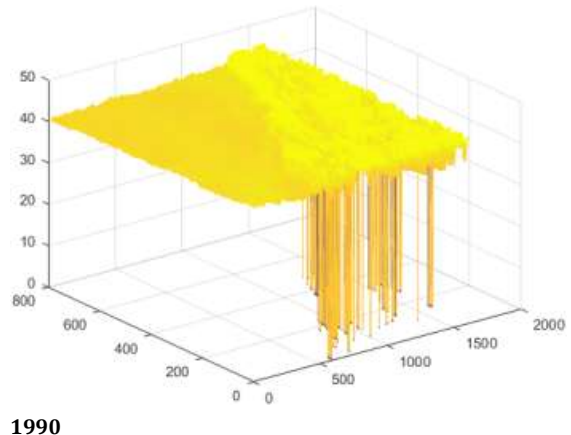
2018

Figure 3. The 3D representation of the NDVI for the study area for the adopted years

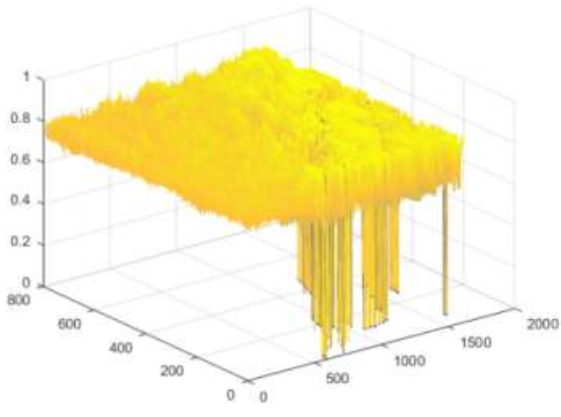
Figure 4. The 3D representation of the NDMI for the study area for the adopted years



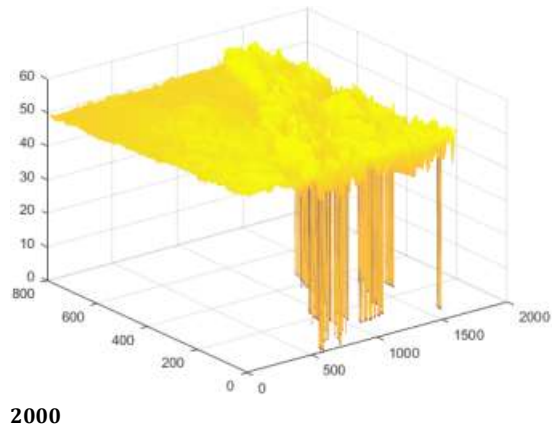
1990



1990

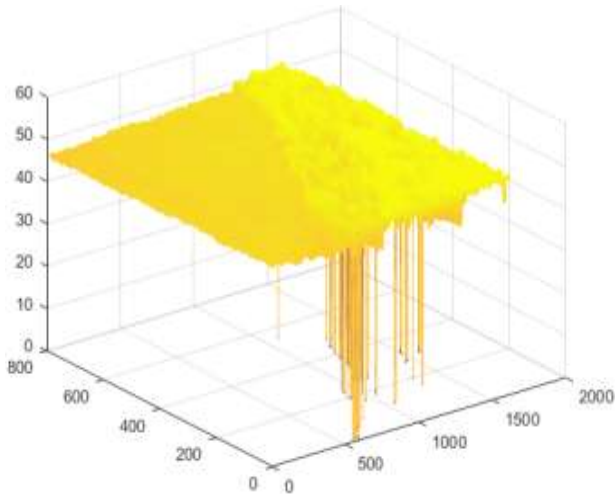


2000

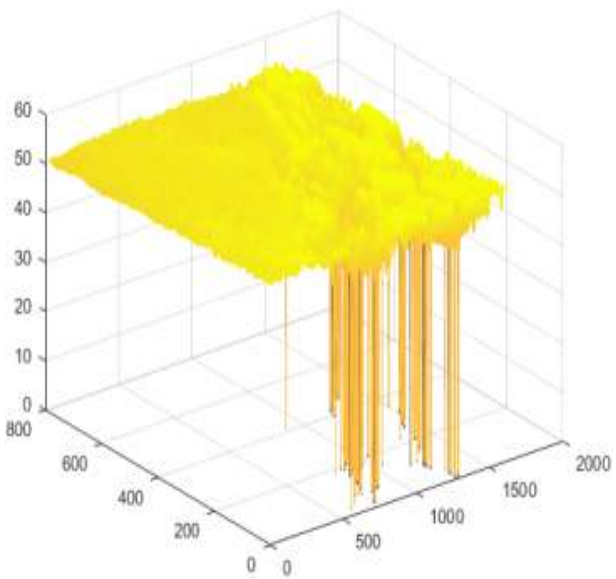


2000





2010



2018

Figure 5. The 3D representation of the TOA temperature for the study area for the adopted years

By excluding the water bodies indices, the land cover indices statistics is illustrated in Table1.

Table 1. The statistics of the soil's indices

Index	NDVI			NMDI			TEMPERATURE		
	Min	Mean	Max	Min	Mean	Max	Min	Mean	Max
1990	0.50	0.51	0.99	0.39	0.77	1.75	28	42	48
2000	0.30	0.33	0.78	0.38	0.78	1.54	33	51	58
2010	0.30	0.31	0.79	0.09	0.63	2.37	30	48	54
2018	0.18	0.19	0.49	0.69	0.78	1.23	35	52	59

The statistics values in Table1 cannot be used to

build the inference system since if include singular points that do not represent the real active range for these indices. By eliminating the singular points and keep the indices ranges to the active value that represent the real behavior, the active ranges of the land cover indices determined as is illustrated in Table 2.

Table 2. The indices active range of the study area soil

Index	NDVI		NMDI		Temp	
	Min.	Max.	Min.	Max.	Min.	Max.
1990	0.46	0.57	0.62	0.86	36	45
2000	0.28	0.41	0.63	0.9	43	57
2010	0.26	0.43	0.52	0.72	43	54
2018	0.17	0.28	0.52	0.79	45	57

In order to build a fuzzy inference system(FIS), the land cover status is divided into six types that represented by a number, as illustrated in Table 3.

Table 3. The fuzzy decision keys for the land cover status

Rules Key	
High Desertification	1
Medium Desertification	2
Low Desertification	3
Low Vegetation	4
Medium Vegetation	5
High Vegetation	6

To define each land cover status, the following decision rules are adopted based on the land cover indices value, as illustrated in Table 4.

Table 4. The decision rules to define the land cover status

Rule	NDVI		NMDI		Temp.		Decision
1	Low	and	Low	and	Low	then	2
2	Low	and	Low	and	High	then	1
3	Low	and	High	and	Low	then	3
4	Low	and	High	and	High	then	3
5	High	and	Low	and	Low	then	5
6	High	and	Low	and	High	then	4
7	High	and	High	and	Low	then	6
8	High	and	High	and	High	then	5

A Mamdani FIS with three input variables that represent the land cover indices and one output variable that represent the land cover status is adopted in this research, as illustrated in Figure6.



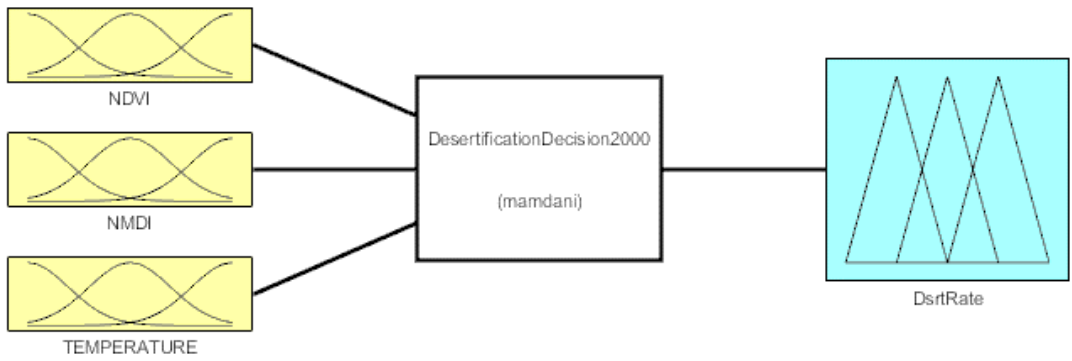
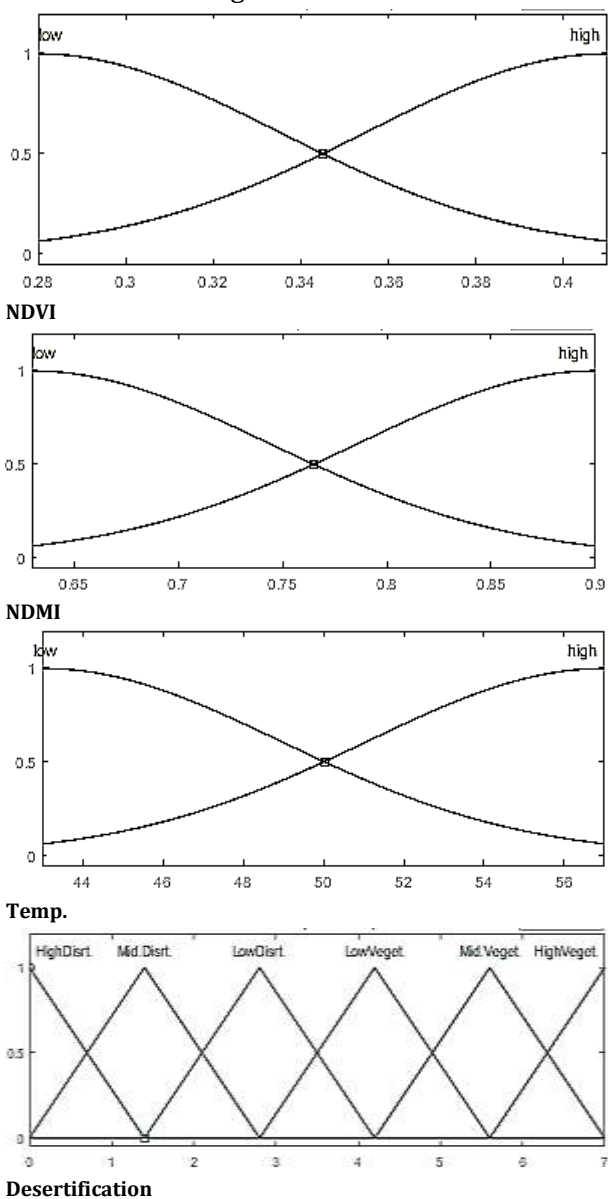


Figure 6. The fuzzy inference system

The active ranges are applied for each land cover index in the FIS, Gaussian member functions are used with the all input variables and a triangle member function is used with the output variable as illustrated in Figure7.



**Desertification**

Figure 7. The FIS inputs and output member functions

According to the input and output member

functions and the decision rule used in the FIS, the decision surfaces are built to determine the land cover status for each year that adopted in this study. The produced decision surfaces for all elected years are very similar in shape but they differ in range, as a sample of the obtained decision surfaces, the decision surface for the year 2000 is illustrated in Figure8.

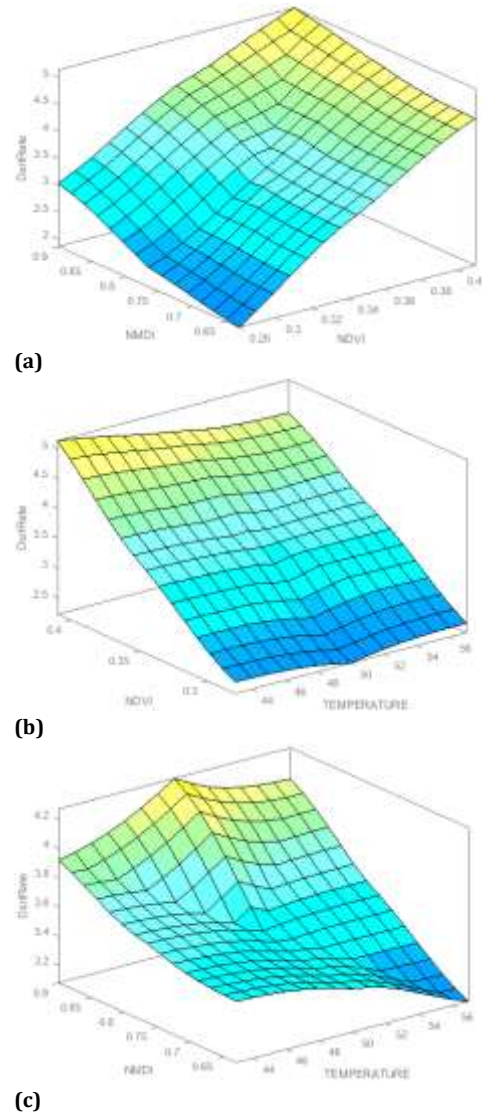


Figure 8. The decision surface for the year 2000 a) NMDI with NDVI b) NDVI with temperature c) NMDI with Temperature

7



By applying the decision surface for each year on the land cover indices, the decision value is calculated as a real number with a fraction part,

therefore, a quantization step is necessary to convert the decision value to an integer value, as is illustrated in the Figures 9 & 10.

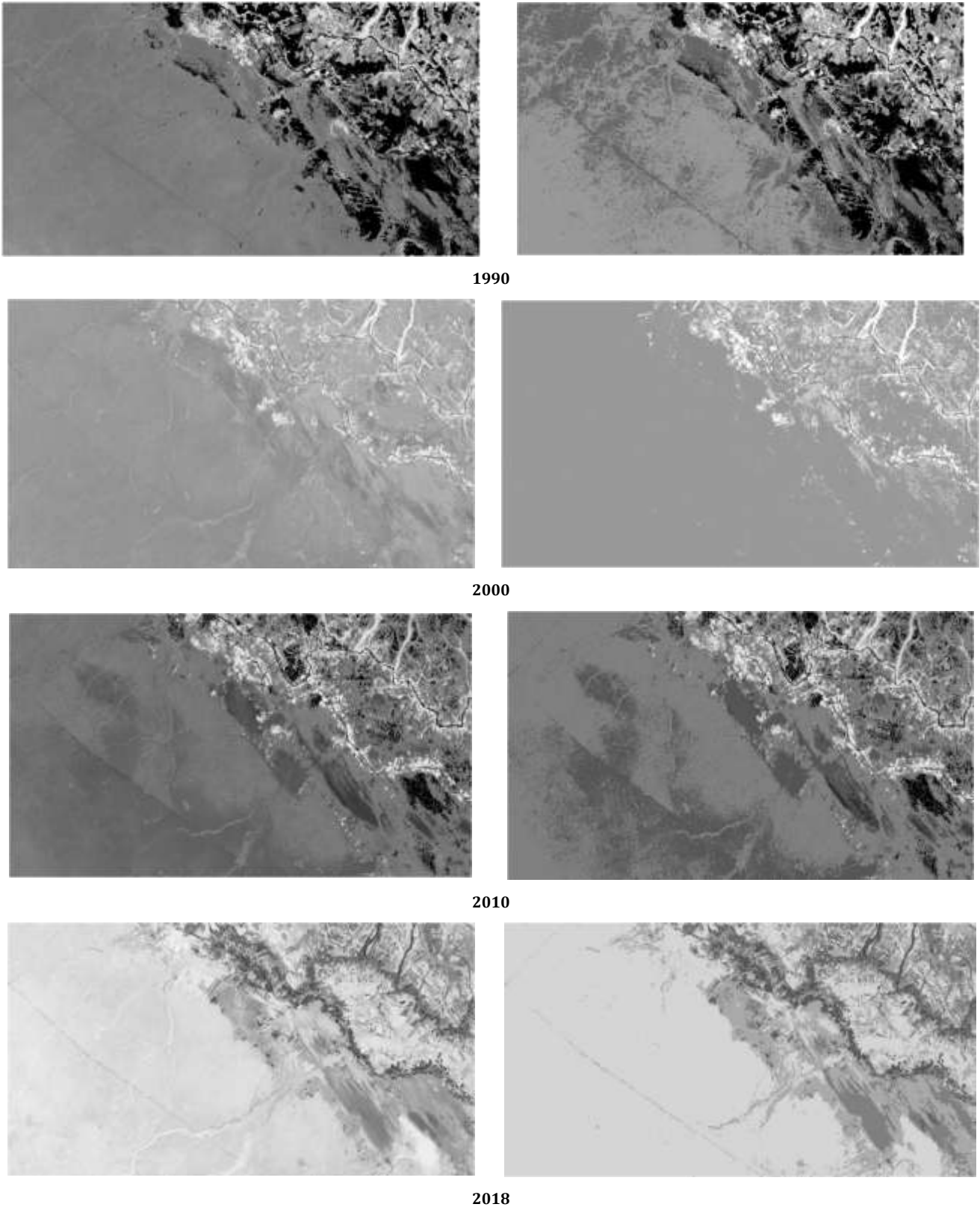


**Figure 9.** The image of the desertification decision values for each year a) before quantization b) after quantization



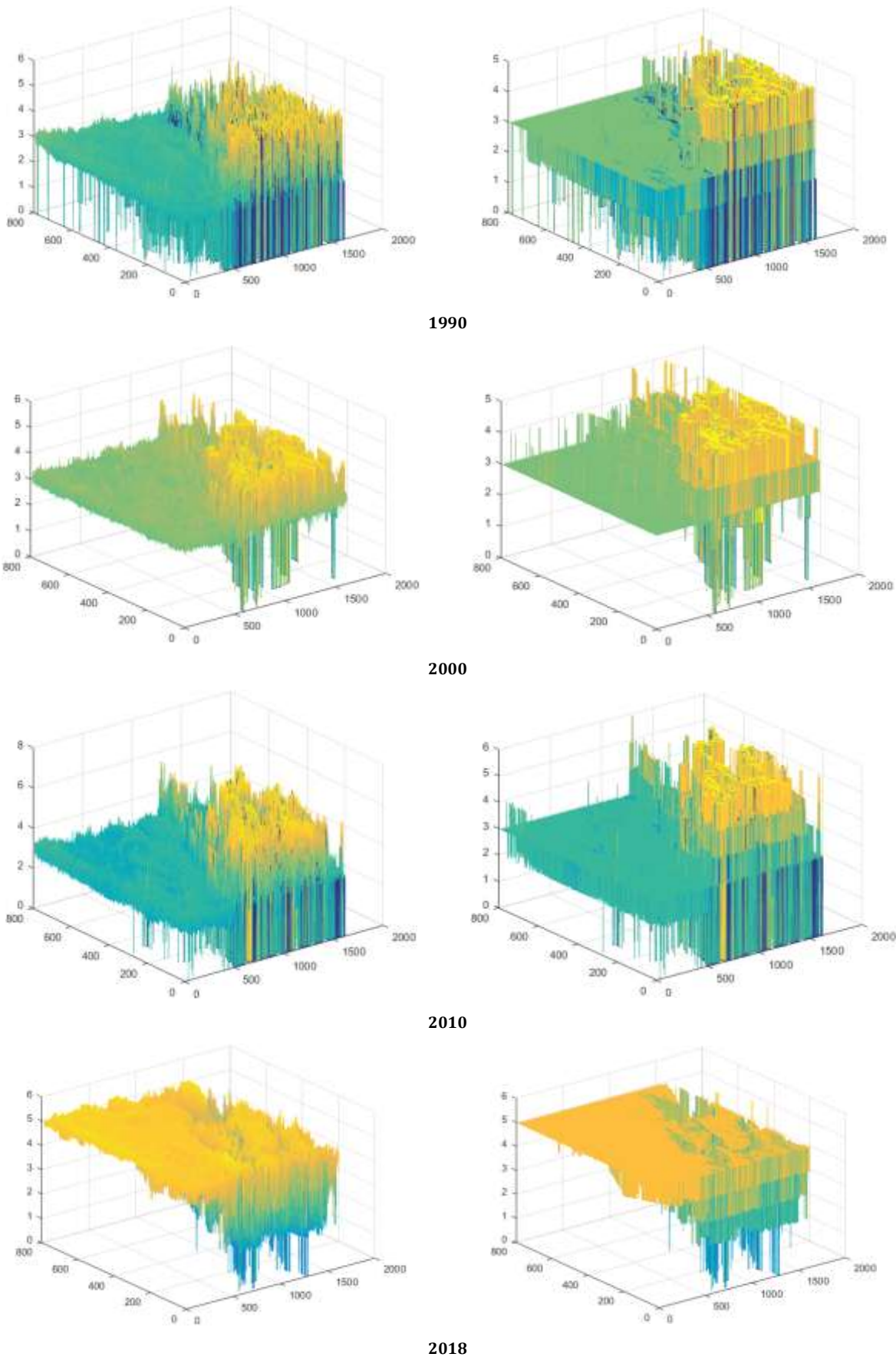


**Figure 10.** 3D representation of desertification decision value for each year where the left column before quantization and right column after quantization



According to the FIS, the study area classified to six categories where the area of each class is calculated for each year as illustrated in Table 5.

**Table 5.** The area of the classified soil according to the decision value

Class / Area	1990 (Km <sup>2</sup> )	2000 (Km <sup>2</sup> )	2010 (Km <sup>2</sup> )	2018 (Km <sup>2</sup> )
High Desertification	0	0	5.175	0.0585
Medium Desertification	357.1047	2.1411	273.2526	46.935
Low Desertification	562.3956	990.6912	720.7641	127.6614
Low Vegetation	50.7933	129.393	49.8159	236.4453
Medium Vegetation	16.5474	26.3313	44.1243	737.5491
High Vegetation	0	0	5.715	0.0387
Water Bodies	162.135	0.4194	50.1291	0.288

The classification results using the FIS recorded the following notes:

- After the year 2000, the high desertification and the high vegetation began to be recorded.
- The area of water bodies is fluctuating, with the highest value recorded in 2010 and the lowest value in 2000.
- Medium vegetation, in general, is in increasing rate.

To evaluate the overall land cover status, Table 6 reflects the overall area for the three major class (desertification, vegetation and water bodies), in which it is obvious that the water bodies are in decreasing rate with time while the desertification is the dominated status before the year 2018. In 2018, it is a turning point in the case of land cover. Although there are few water bodies, the vegetation rate has increased dramatically at the expense of desertification as shown in Figure 11. The decrease in the area of water masses did not affect the increase in the recorded areas of vegetation, which indicates an increase in the amount of rain that contributed to this

**Table 6.** The overall land cover area

Class / Area	1990 (Km <sup>2</sup> )	2000 (Km <sup>2</sup> )	2010 (Km <sup>2</sup> )	2018 (Km <sup>2</sup> )
Desertification	919.5003	992.8323	999.1917	174.6549
Vegetation	67.3407	155.7243	99.6552	974.0331
Water Bodies	162.135	0.4194	50.1291	0.288

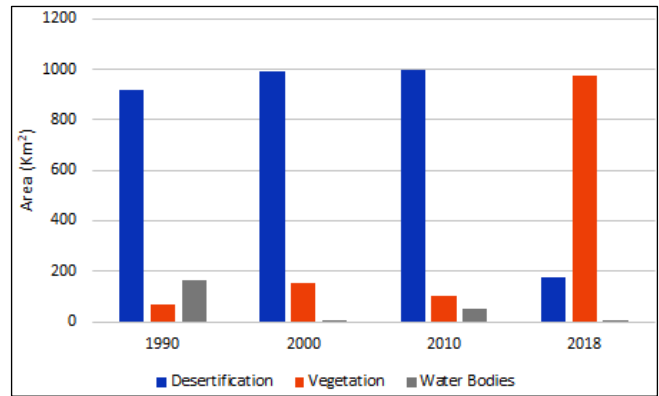


**Figure 11.** The overall area for the land cover status

### Conclusion

In this research, the use of the FIS to classify the marshland of Iraq give us closer result to the humane definition of desertification by using three land cover indices. The results indicate that the medium vegetation class is in increasing for all the years that adopted and the desertification is reduced dramatically in the year 2018 in spite of that the water bodies area is unchanged.

### References

Shoba P, Ramakrishnan SS. Modeling the contributing factors of desertification and evaluating their relationships to the soil degradation process through geomatic techniques. *Solid Earth* 2016; 7(2): 341-354.

Adhikary PP, Dash CJ, Sarangi A, Singh DK. Hydrochemical characterization and spatial distribution of fluoride in groundwater of Delhi state, India. *Indian Journal of Soil Conservation*, 2014; 42(2): 170-173.

Moridnejad A, Karimi N, Ariya PA. Newly desertified regions in Iraq and its surrounding areas: Significant novel sources of global dust particles. *Journal of Arid Environments*, 2015; 116: 1-10.

Mail AASM. Desertification detected in the Udhaim River Basin, Iraq based on spectral indices derived from remote sensing images. *Miscellanea Geographica*, 2017; 21(3): 124-131.

Torres L, Abraham EM, Rubio C, Barbero-Sierra C, Ruiz-Pérez M. Desertification research in Argentina. *Land Degradation & Development* 2015; 26(5): 433-440.

Miao L, Moore JC, Zeng F, Lei J, Ding J, He B, Cui X. Footprint of research in desertification management in China. *Land Degradation & Development* 2015; 26(5): 450-457.

Naji TA, Hatem AJ. New Adaptive Satellite Image Classification Technique for Al habbinya Region West of Iraq. *Ibn AL-Haitham Journal For Pure and Applied Science* 2017; 26(2): 143-149.

Ziboon ART, Alwan IA, Khalaf AG. Study and analysis of desertification phenomenon in Karbala governorate by remote sensing data and GIS. *Iraqi Bulletin of Geology and Mining*, 2015; 11(1): 143-156.

Awda GJ. Spatial analysis of desertification phenomenon using remote sensing and geographic information system (GIS) technology Northwest Wasit Province /Iraq - a case study



- Ghassan Jamil Awda. Journal of Wassit For Science & Medicine, 2015; 8(2): 39-53.
- Geerken R, Iaiwi M. Assessment of rangeland degradation and development of a strategy for rehabilitation. Remote Sensing of Environment, 2004; 90(4): 490-504.
- Hadeel AS, Jabbar MT, Chen X. Application of remote sensing and GIS in the study of environmental sensitivity to desertification: a case study in Basrah Province, southern part of Iraq. Applied Geomatics 2010; 2(3): 101-112.
- Ali SM, Salman SS. Estimating the Yield of Rice Farms in Southern Iraq using Landsat images. International Journal of Scientific & Engineering Research 2015; 6(8): 1607-1614.
- Wang L, Qu JJ, Hao X. Forest fire detection using the normalized multi-band drought index (NMDI) with satellite measurements. Agricultural and forest meteorology 2008; 148(11): 1767-1776.
- Raheem MA, Hatem AJ. Calculation of Salinity and Soil Moisture indices in south of Iraq-Using Satellite Image Data. Energy Procedia 2019; 157: 228-233.
- Ross TJ. Fuzzy logic with engineering applications. John Wiley & Sons 2005.
- Asaad SH, Mohammed AS. New Properties of Anti Fuzzy Ideals of Regular Semigroups. Ibn AL-Haitham Journal For Pure and Applied Science 2019; 32(3): 109-116.
- Hegde S. Modelling land cover change: A fuzzy approach, M.Sc. thesis, International Institute for Geo Information science and Earth Observation Enschede 2003.
- Mohamed AMO, Hawas Y. Neuro-Fuzzy Logic Model for Evaluating Water Content of Sandy Soils. Computer-Aided Civil and Infrastructure Engineering 2004; 19(4): 274-287.
- Sharma M, Gupta R, Kumar D, Kapoor R. Efficacious approach for satellite image classification. Journal of Electrical and Electronics Engineering Research 2011; 3(8): 143-150.
- Shah P, Vayada MG. Review on Satellite Image Classification using Fuzzy Logic. International Journal of Science and Research, 2015; 4(12): 1245-1248.
- Taufik A, Ahmad SSS. Land cover classification of Landsat 8 satellite data based on Fuzzy Logic approach. In IOP Conference Series: Earth and Environmental Science IOP Publishing 2016; 37(1): 012062.
- Earth Explorer - Home, U.S.G. Survey, [Online]. Available: <http://earthexplorer.USGS.gov>. 2019.
- Buringh P. Exploratory Soil Map of Iraq, Division of Soil and Agricultural Research and Projects, Ministry of Agriculture, Baghdad, Iraq 1957.
- Zanter K. Landsat 8 (L8) data users handbook, Department of the Interior US Geological survey 2019.
- Wang L, Qu JJ. NMDI: A normalized multi-band drought index for monitoring soil and vegetation moisture with satellite remote sensing. Geophysical Research Letters 2007; 34(20): 1-5.
- Giannini MB, Belfiore OR, Parente C, Santamaria R. Land Surface Temperature from Landsat 5 TM images: comparison of different methods using airborne thermal data. Journal of Engineering Science & Technology Review 2015; 8(3).
- Tan K, Liao Z, Du P, Wu L. Land surface temperature retrieval from Landsat 8 data and validation with geosensor network. Frontiers of Earth Science 2017; 11(1): 20-34.

